Antitumor and immunomodulatory effects of a novel multitarget inhibitor, CS2164, in mouse hepatocellular carcinoma models

You Zhou, Chao Fu, Yidi Kong, Desi Pan, Yanan Wang, Shengjian Huang, Zhibin Li, Zhiqiang Ning, Xianping Lu, Song Shan and Lijun Xin

As a novel orally active multitarget small molecule inhibitor, CS2164 has shown broad antitumor activities against several human tumor xenograft models in immune-compromised mice. However, the ability of CS2164 to modulate antitumor immunity in an immune-competent mouse tumor model remains undefined, although antiangiogenic treatment has been reported to affect immune cell infiltration and remodel the tumor immune microenvironment. In the present study, the subcutaneous and ascites hepatocellular carcinoma (HCC) models in syngeneic Balb/c mice established by inoculation of an H22 hepatoma cell line were utilized to investigate the antitumor and immunomodulatory effects of CS2164. Although the antitumor effects of CS2164 were validated in both subcutaneous and ascites HCC models in syngeneic mice, CS2164 treatment consistently modulated immune cell populations, both in the periphery and in tumor microenvironments, with upregulation of $CD4^+$ and $CD8^+$ T cells in the spleen, but downregulation of immunosuppressive populations including regulatory T cells, myeloid-derived suppressor cells, and tumor-associated macrophages in the spleen and tumor tissues. Furthermore, CS2164 increased the relative gene expression and protein production of several proinflammatory cytokines in tumor-related ascites. These results indicate that CS2164 exerts an antitumor effect associated with its immunomodulatory activities in mouse HCC models, and may also provide evidence for the immunotherapy potentiation of CS2164 in future cancer treatment. *Anti-Cancer Drugs* 30:909–916

Anti-Cancer Drugs 2019, **30**:909–916

Keywords: antitumor, CS2164, hepatocellular carcinoma, immunomodulation, myeloid-derived suppressor cell, multitarget inhibitor, proinflammatory cytokine, regulatory T cell, tumor-associated macrophage

Shenzhen Chipscreen Biosciences Co. Ltd., Shenzhen, Guangdong, China

Correspondence to Lijun Xin, PhD, Shenzhen Chipscreen Biosciences Co. Ltd., BIO-Incubator, Suit 2-603B, Shenzhen Hi-Tech Industrial Park, Shenzhen, Guangdong 518057, China
Tel: +86 755 2695 2126; fax: +86 755 2695 7291;
e-mail: xinlijun@chipscreen.com

Received 25 January 2019 **Revised form accepted** 24 March 2019

Introduction

Hepatocellular carcinoma (HCC) remains a leading cause of cancer-related mortality, with the 5-year overall survival being only 10% [1]. Ascites is often observed in HCC patients and may be associated with decreased long-term survival [2]. To date, the only approved treatment options for patients with advanced HCC are antiangiogenic drugs such as sorafenib and regorafenib and recently the immune checkpoint inhibitor nivolumab (approved in the USA only) [3–5]. Particularly, the CheckMate 040 trial reported promising results for nivolumab, with response rates of ~20% and durable responses for patients who had already been treated or were intolerant to sorafenib, indicating more effective and superior clinical benefits of immunotherapy in HCC treatment.

Interestingly, proangiogenic cytokines, such as vascular endothelial growth factors (VEGFs), have been known to play a major role in shaping tumor-associated immunosuppression besides promoting tumor growth [6,7]. Furthermore, blockade of the VEGF/VEGFR signaling pathway by targeted tyrosine kinase inhibitors or antibodies has also yielded improved antitumor immunity in both animal models and patients [8–12]. Thus, normalization of the tumor vasculature by antiangiogenic treatment not only enhances tissue perfusion but also improves immune effector cell infiltration and remodels the tumor immune microenvironment, leading to immunotherapy potentiation for cancer treatment [13].

CS2164 is a novel orally active multitarget small molecule inhibitor that simultaneously inhibits three major pathways in tumorigenesis, including the angiogenesis-related kinases (VEGFR2, VEGFR1, VEGFR3, PDGFRα, and c-Kit), the mitosis-related kinase, Aurora B, and the chronic inflammation-related kinase, CSF-1R. The compound shows very high selectivity and potency in the inhibition of these kinases, with the IC_{50} values in the single-digit nanomolar range [14]. In preclinical studies, CS2164 has shown broad and dose-dependent antitumor activities against several human tumor xenograft models

0959-4973 Copyright © 2019 The Author(s). Published by Wolters Kluwer Health, Inc. DOI: 10.1097/CAD.0000000000000791

in immune-compromised mice [14]. However, it remains unclear whether CS2164 can modulate antitumor immunity in immune-competent mouse tumor models.

In this study, the antitumor effects of CS2164 were investigated in both subcutaneous and ascites HCC models in syngeneic mice. Furthermore, the immunomodulatory activities of CS2164 were examined through the analyses of several immune cell populations in both peripheral immune organ and tumor tissues.

Materials and methods

Mice, cell line, and compound

Female Balb/c mice at 6–8 weeks old were purchased from the Animal Experimental Center (Guangzhou, China) and accommodated for 1 week before the experiment. A murine H22 hepatoma cell line derived from Balb/c mice was purchased from the China Center for Type Culture Collection (Wuhan, Hubei, China). H22 cells were cultured in RPMI-1640 medium supplemented with 2 mmol/l L-glutamine, 100 IU/ml penicillin, 100 μg/ml streptomycin, and 10% fetal calf serum at 37°C under a humidified atmosphere of 5% CO_2. CS2164 was synthesized by Shenzhen Chipscreen Biosciences Co. Ltd (Shenzhen, China). For in-vivo administration, CS2164 (10 mg/kg) was dissolved in a 0.2% (w/v) carboxymethyl cellulose sodium suspension for oral gavage once daily, with 0.2% (w/v) carboxymethyl cellulose sodium suspension as the vehicle control. All animal experiments were reviewed and approved by the Institutional Animal Care and Use Committee of Shenzhen Chipscreen Biosciences Co. Ltd.

Hepatocellular carcinoma subcutaneous and ascites models

Naive Balb/c mice were inoculated subcutaneously with H22 cells (1×10^6 cells in 100 μl PBS per mouse) in the lower back [15]. One day after inoculation, mice were grouped randomly and treated intragastrically with vehicle or CS2164 (10 mg/kg) once daily. Tumor development was monitored every 2 days from day 8 until termination of the experiments. The tumor volume (mm^3) was calculated using the modified ellipsoidal formula of ($width^2 \times length$)/2 on the basis of caliper measurement [16]. Animal body weights were also monitored daily during treatment. After treatment for 2 weeks, all the mice were killed humanely. Tumor tissues were isolated, weighed, and then subjected to the isolation of tumor-infiltrating cells. Mouse splenocytes were isolated and stained for analyses of immune cell populations by flow cytometry.

An ascites model of HCC was established according to the previous study [17]. In brief, Balb/c mice were inoculated intraperitoneally with H22 cells (3×10^6 cells in 100 μl PBS per mouse) into the left lower abdomen. Mice were then randomized into two groups and treated intragastrically with vehicle or CS2164 (10 mg/kg), once daily. Animal body weights were monitored daily during treatment. At day 8, mouse abdomen became obviously distended, all the animals were killed humanely, and the ascitic fluid was collected directly using a syringe. For tumor cell morphology, a drop of the cell-containing ascitic fluid from the control and CS2164-treated mice was directly smeared on glass slides and stained with Wright–Giemsa dye (Sangon Biotech, Shanghai, China). Then, after centrifugation of the ascitic fluid at 300*g* at room temperature for 10 min, the supernatant of the ascites was collected. The total volume of ascitic fluid was calculated and cytokines in the supernatant of the ascites were measured using an enzyme-linked immunosorbent assay (ELISA).

In a separate experiment, to thoroughly collect and calculate the total number of the ascitic cells, 5 ml of PBS solution per mouse were injected intraperitoneally before extraction of ascites. Tumor cells in the ascites were counted, and the ascitic immune cell populations were stained with the indicated markers and analyzed by flow cytometry. Around 1×10^7 of total ascitic cells from both groups were subjected to RNA extraction, followed by a quantitative reverse transcription PCR analysis.

Isolation of tumor-infiltrating lymphocytes

Tumor-infiltrating cells were isolated from tumor tissue by density gradient centrifugation as described previously [18]. Briefly, H22 tumor tissues were minced and digested with 0.5 mg/ml collagenase IV (Sigma-Aldrich, St Louis, Missouri, USA) and 0.1 mg/ml DNase I (Roche, Basel, Switzerland) in RPMI-1640/5% fetal calf serum for 1 h at 37°C. The cell suspension was then filtered through a 70-mm nylon mesh, layered on a Percoll gradient (30–70%), and centrifuged for 20 min. The separated tumor-infiltrating lymphocyte fraction was then collected and washed twice before staining with the indicated cell surface markers.

Monoclonal antibodies and flow cytometry

The following fluorochrome-conjugated anti-mouse monoclonal antibodies for cell surface markers and intranuclear factor were purchased from eBiosciences (San Diego, California, USA): fluorescein isothiocyanate-conjugated anti-CD4 (cat no. 11-0041-85), anti-Gr-1 (cat no. 11-5931-82), anti-MHC-II (cat no. 11-5321-82); phycoerythrin-conjugated anti-CD45 (cat no. 12-0451-83), anti-CD25 (cat no. 12-0251-83); phycoerythrin cyanine7-conjugated anti-CD8 (cat no. 25-0081-82), anti-F4/80 (cat no. 25-4801-82); allophycocyanin (APC)-conjugated anti-CD11b (cat no. 17-0112-82), and anti-Foxp3 (cat no. 17-5773-82). Single-cell suspensions of splenocytes, tumor-infiltrating lymphocytes, and ascitic cells were stained on ice for 30 min with the indicated cell surface marker antibodies (dilution, 1: 200). For intranuclear Foxp3 staining, cells were fixed and permeabilized using a Cytofix/Cytoperm Kit (cat no. 00-5523-00;

eBiosciences) on ice for 30 min after labeling with surface marker antibodies, followed by anti-Foxp3 mAb (dilution, 1: 50) intranuclear staining on ice for 30 min. Samples were acquired on a BD FACScanto II flow cytometer (BD Biosciences, San Jose, California, USA) and the results were analyzed using Flowjo software (TreeStar, Ashland, Oregon, USA).

Quantitative reverse transcription PCR analysis

The total RNA from ascitic cells was isolated by TRIzol reagent according to the manufacturer's instructions (Ambion, Austin, Texas, USA). Five miocrogram of extracted RNA was reverse transcribed into cDNA first-strand using the Transcriptor First Strand cDNA Synthesis Kit (Roche Diagnostics, Mannheim, Germany). Synthesized cDNA was diluted 50 times with nuclease-free water before the quantitative real-time PCR analyses. Quantitative PCR was performed with the ABI Prism 7000 Sequence Detection System (Applied Biosystems, Foster City, California, USA) using SYBR Green Master (ROX) dye (Roche Diagnostics), and threshold cycle numbers were obtained using ABI Prism 7000 SDS software, version 1.0. The amplification condition consisted of a preincubation at 94°C for 3 min, followed by 40 cycles of 94°C for 10 s, 55°C for 10 s, and 72°C for 10 s, and then one cycle of 72°C for 10 min All reactions were followed by melting curve analysis and performed in triplicate. The primer sequences used in this study are listed below: *IFN-γ*, forward: 5′-CTTCAGCAACAGCAAGGCG-3′ and reverse: 5′-CAGCGACTCCTTTTCCGCTT-3′; *TNF-α*, forward: 5′-TGATCGGTCCCCAAAGGGAT-3′ and reverse: 5′-GCTACGACGTGGGCTACAGG-3′; *IL-6*, forward: 5′-GGAGCCCACCAAGAACGATAG-3′ and reverse: 5′-GTGAAGTAGGGAAGGCCGTG-3′; *IL-17* forward: 5′-ACTACCTCAACCGTTCCACG-3′ and reverse: 5′-TTCCCTCCGCATTGACACAG-3′; β-actin, forward: 5′-GACGTTGACATCCGTAAAGAC-3′ and reverse: 5′-CCACCGATCCACACAGAGT-3′. The relative expression of cytokine genes was normalized to the internal control, the β-actin gene, and analyzed using the $2^{-\Delta\Delta C_q}$ method [19].

Cytokine measurement by enzyme-linked immunosorbent assay

Cytokine [interferon-γ (IFN-γ) and interleukin-6 (IL-6)] concentrations in the supernatant of the ascites from the vehicle control and CS2164-treated mice were determined using mouse cytokine high-sensitivity ELISA kits according to the manufacturer's protocols (Multisciences Biotech, Hangzhou, China).

Statistical analysis

All data were analyzed and represented as the mean ± SD using GraphPad Prism software (GraphPad Software, La Jolla, California, USA). Student's *t*-test was used for comparison of the mean values between two groups. A *P* value of less than 0.05 was considered statistically significant.

Results

Inhibition of hepatocellular carcinoma tumor growth by CS2164 in a syngeneic mouse xenograft model

To evaluate the effect of CS2164 on the growth of HCC cells *in vivo*, a syngeneic mouse xenograft model, in which

Fig. 1

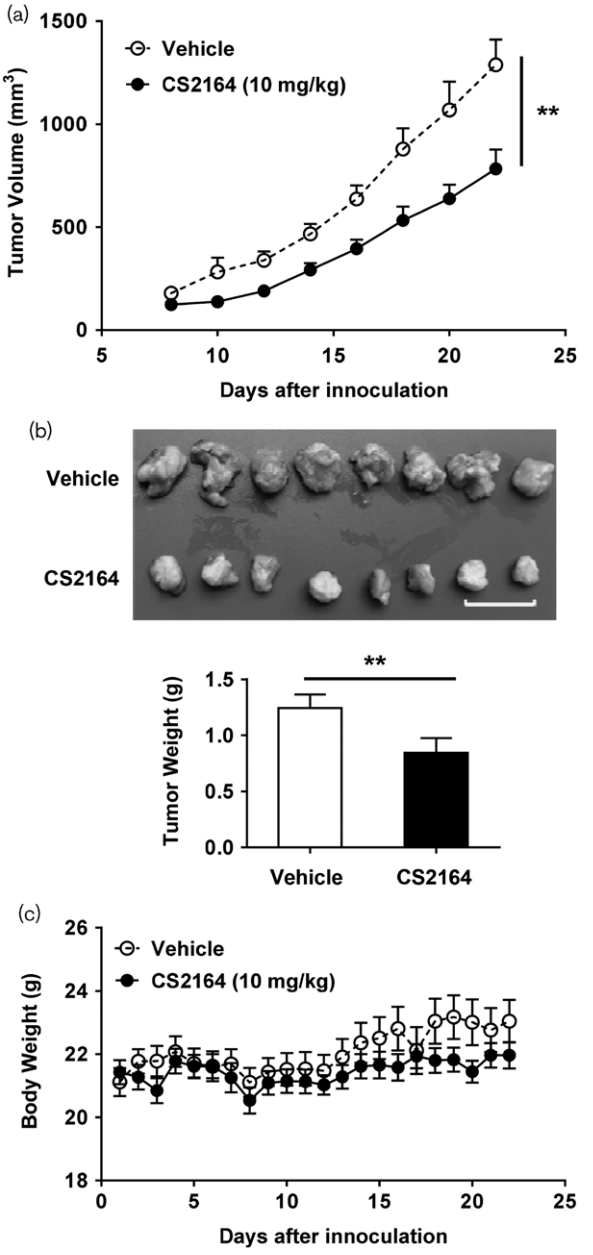

CS2164 inhibits tumor growth in a subcutaneous hepatocellular carcinoma (HCC) model. The syngeneic Balb/c mice were inoculated subcutaneously with 1×10^6 H22 cells. One day after inoculation, mice were randomized into two groups (n=8–10 mice/group) and administered intragastrically with either vehicle control or CS2164 (10 mg/kg), once daily. Tumor volumes (a), isolated tumor tissues (scale bar, 2 cm) and tumor weights at day 22 (b), and animal body weights (c) from each group are shown. The representative data are expressed as mean ± SD from one of two independent experiments. $^{**}P<0.01$ compared with the vehicle control group.

Balb/c mice were inoculated subcutaneously with the H22 hepatoma cell line generated previously from Balb/c mice, was utilized. One day after inoculation, tumor-bearing mice were randomized into two groups and administered intragastrically with vehicle or CS2164 (10 mg/kg) once daily. CS2164 significantly inhibited tumor growth, with a mean tumor volume of 784 ± 93 mm^3 in the CS2164-treated group compared with 1288±124 mm^3 in the vehicle control ($P < 0.01$; Fig. 1a), and a mean tumor weight of 0.84±0.13 g in the CS2164-treated group compared with 1.24 ± 0.12 g in the vehicle control at the end of the experiments at day 22 ($P < 0.01$; Fig. 1b). The relatively stable body weights in CS2164-treated mice were also well correlated with reduced tumor growth rather than any drug-related adverse effect (Fig. 1c). Thus, CS2164 exerts antitumor effects in a syngeneic mouse HCC model.

Modulation of immune cell populations by CS2164 in hepatocellular carcinoma tumor-bearing mice

Previous studies have shown that VEGF/VEGFR antagonists modulate T effector and Treg cells in HCC patients and mouse models of colorectal carcinoma [9,12]. To investigate the potential of CS2164 to also have immunomodulatory activity, as the VEGFRs signaling pathway is one of its major targets, the frequencies of several peripheral immune cell populations were studied by flow cytometry. Compared with the vehicle control, treatment with CS2164 significantly increased the frequencies of $CD4^+$ and $CD8^+$ T-cell populations in the spleen of tumor-bearing mice (Fig. 2a). Correspondingly, the $CD25^+$ $Foxp3^+$ Tregs frequency was significantly decreased (Fig. 2b), which may indicate the reversal of immune suppression in the periphery.

As VEGF/VEGFRs and CSF-1/CSF-1R signaling pathways are also involved in the infiltration and/or proliferation of myeloid-derived suppressor cells (MDSCs) and tumor-associated macrophages (TAMs) [20–23], the impact of CS2164 on these two cell populations was further investigated. Compared with the vehicle control, treatment with CS2164 significantly reduced the frequencies of $CD11b^+$ $Gr\text{-}1^+$ MDSCs, both in the spleen (Fig. 3a) and in the infiltrating $CD45^+$ lymphocytes of tumor tissue (Fig. 3b). Furthermore, $F4/80^+$ $MHC\text{-}II^+$ TAMs that gated on $CD45^+$ $CD11b^+$ tumor-infiltrating lymphocytes were also significantly decreased by CS2164 (Fig. 3c). Therefore, CS2164 has immunomodulatory impacts on both peripheral and tumor tissue immune cell populations.

Antitumor and immunomodulatory effects of CS2164 in the hepatocellular carcinoma ascites model

Next, to further verify the immunomodulatory effects of CS2164, particularly on tumor-infiltrating immune cells,

Fig. 2

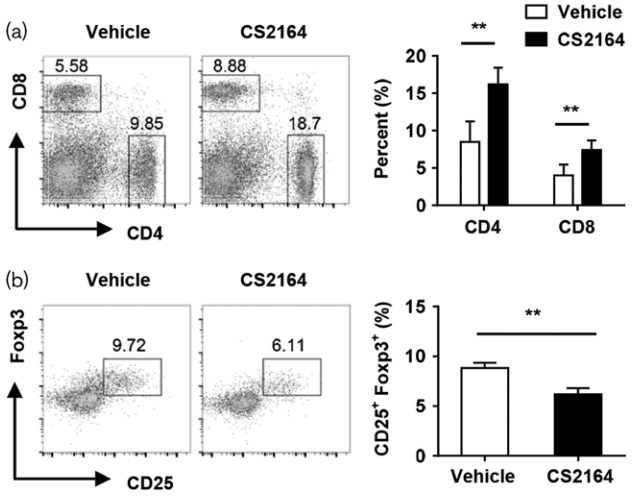

CS2164 affects the frequencies of T-cell subpopulations in the spleen. The frequencies of $CD4^+$ and $CD8^+$ T cells (a) and $CD25^+$ $Foxp3^+$ Tregs (b) in the spleen from vehicle-treated or CS2164-treated mice described in Fig. 1 were analyzed by flow cytometry. The representative plots are shown and the accumulative data are expressed as mean ± SD from one of two independent experiments. $^{**}P < 0.01$ compared with the vehicle control group.

Fig. 3

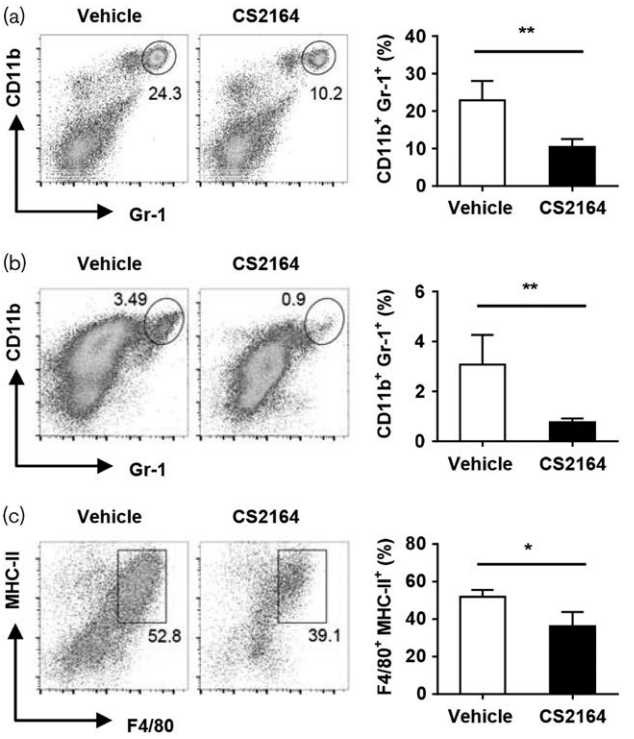

CS2164 decreases the frequencies of MDSCs and TAMs in both spleen and tumor tissue. The frequencies of spleen (a), $CD11b^+$ $Gr\text{-}1^+$ MDSC cells (b), and $F4/80^+$ $MHC\text{-}II^+$ TAMs (c) in tumor tissues from vehicle-treated or CS2164-treated mice described in Fig. 1 were analyzed by flow cytometry. The representative plots are shown and the accumulative data are expressed as mean ± SD from one of two independent experiments. $^{*}P < 0.05$; $^{**}P < 0.01$ compared with the vehicle control group. MDSC, myeloid-derived suppressor cell; TAM, tumor-associated macrophage.

Fig. 4

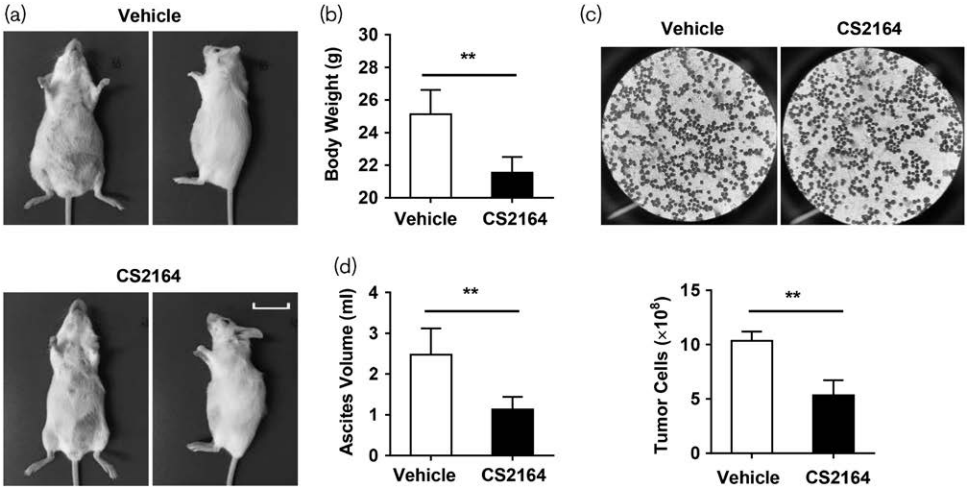

The antitumor effect of CS2164 in a hepatocellular carcinoma (HCC) ascites model. Balb/c mice were inoculated intraperitoneally with 3×10^6 H22 cells. Mice were randomized into two groups ($n=5$ mice/group) and administered intragastrically with either vehicle control or CS2164 (10 mg/kg) once daily. (a) The representative photos of the ascitic mouse model from each group are shown. Scale bar, 2 cm. Animal body weights (b), tumor cell morphology (c), ascites volume, and total tumor cells in the ascites (d) at day 8 are shown. The representative data are expressed as mean ± SD from one of two independent experiments. $^{**}P<0.01$ compared with the vehicle control group.

the HCC ascites mouse model established by an intraperitoneal inoculation of H22 cells was used. As shown in Fig. 4, treatment with CS2164 in HCC ascites mice clearly inhibited the distended abdomen, with significantly decreased body weights compared with the vehicle control (Fig. 4a and b). Although tumor cells in the ascites from the vehicle control and CS2164-treated mice were not morphologically different (Fig. 4c), CS2164 significantly reduced both the ascites volume and the total tumor cells in the ascites to over half of those in the vehicle-treated mice (Fig. 4d).

The immune cell populations in the ascites were then investigated and analyzed by direct staining with the indicated cell markers. Although the tumor-infiltrating $CD45^+$ lymphocytes in the ascites from the vehicle-treated or CS2164-treated mice were comparable and around 3–4% of the total peritoneal cells (Fig. 5a), the frequencies of MDSCs and TAMs among the infiltrating $CD45^+$ lymphocytes were significantly reduced by CS2164 treatment (Fig. 5b and c). Interestingly, both $CD4^+$ and $CD8^+$ T cells in the ascitic lymphocytes from CS2164-treated mice were significantly decreased compared with those in vehicle-treated mice (Fig. 5d), which is likely because of the inhibition of VEGFR3-mediated lymphangiogenesis by CS2164 [24]. Furthermore, $Foxp3^+$ Tregs in ascitic $CD4^+$ T cells were consistently decreased by CS2164 compared with the vehicle treatment (Fig. 5e). Collectively, the antitumor and immunomodulatory effects of CS2164 are further validated in the HCC ascites mouse model.

Increased gene expression and protein production of proinflammatory cytokines in the ascites by CS2164

Finally, to investigate whether the antitumor and immunomodulatory effects of CS2164 were correlated with cytokine changes in tumor tissue, the gene expression and protein production of several proinflammatory cytokines in ascites were measured by real-time quantitative reverse transcription PCR and ELISA, respectively. Compared with the vehicle control, CS2164 treatment significantly increased the relative gene expressions of *IFN-γ*, *TNF-α*, *IL-6*, and *IL-17* from ascitic cells (Fig. 6a). Confirmatively, the protein levels of IFN-γ and IL-6 in the ascites were also increased by CS2164 treatment (Fig. 6b). Thus, the increased levels of proinflammatory cytokines in the tumor microenvironment possibly result from the inhibition of immunosuppressive cell populations, which eventually contributes toward the antitumor effect of CS2164.

Discussion

As a novel multitarget inhibitor, CS2164 inhibits three major pathways involved in tumorigenesis, such as angiogenesis, mitosis, and chronic inflammation. The broad antitumor efficacy of CS2164 has been shown in different xenograft tumor models in immune-compromised mice [14]. In this study, the antitumor effects of CS2164 were further verified in HCC subcutaneous and ascites models in syngeneic mice. The results indicate that CS2164 has modulatory impacts on different immune cell populations in the periphery and tumor tissues, as well as proinflammatory cytokine expression in the tumor microenvironment. Thus, the antitumor effect

Fig. 5

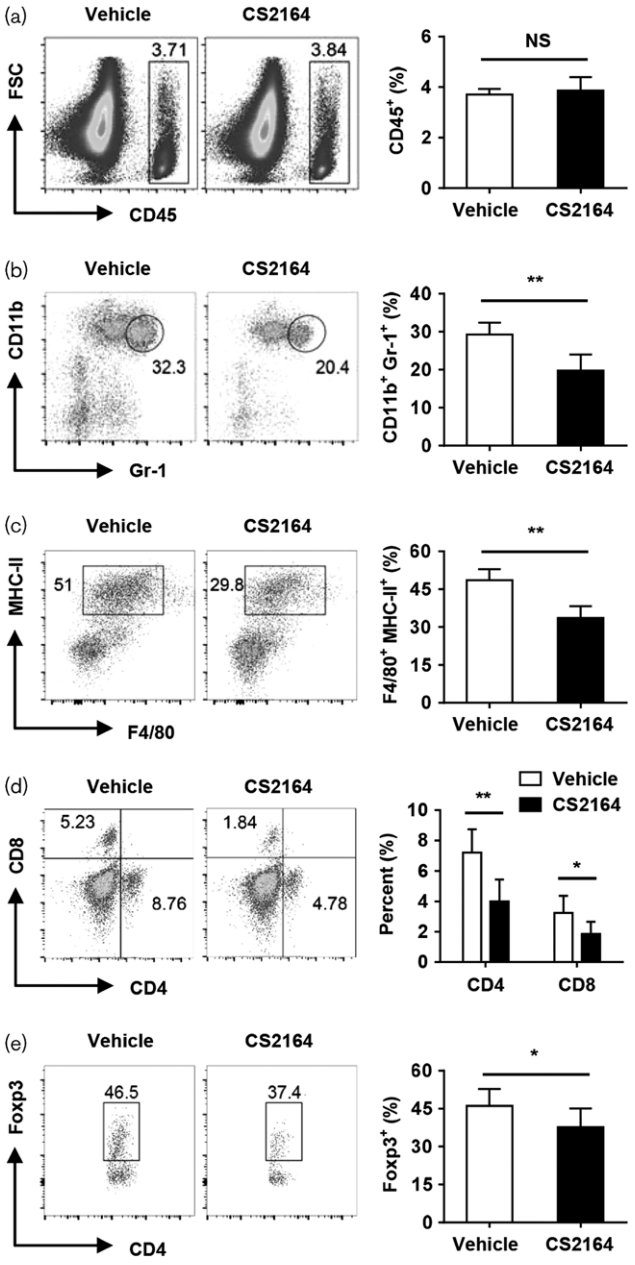

The immunomodulation of different immune cell populations by CS2164 in ascites. The frequencies of $CD45^+$ lymphocytes (a), MDSCs (b), TAMs (c), $CD4^+$ and $CD8^+$ T cells (d), and $Foxp3^+$ Tregs (e) in the ascites from vehicle-treated or CS2164-treated mice described in Fig. 4 were analyzed by flow cytometry. The representative plots are shown and the accumulative data are expressed as mean ± SD from one of two independent experiments. *P<0.05; **P<0.01 compared with the vehicle control group. MDSC, myeloid-derived suppressor cell; TAM, tumor-associated macrophage.

Fig. 6

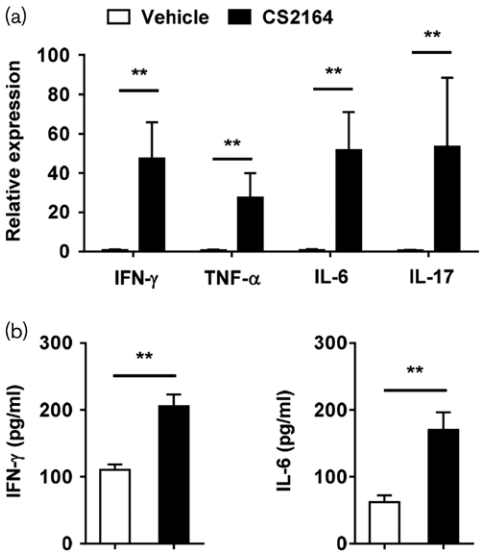

CS2164 increases the relative gene expression and protein production of proinflammatory cytokines. (a) The relative gene expressions of *IFN-γ*, *TNF-α*, *IL-6*, and *IL-17* in ascetic cells from vehicle-treated or CS2164-treated mice described in Fig. 4 were analyzed by quantitative reverse transcription PCR. (b) The protein levels of IFN-γ and IL-6 in the supernatants of the ascites were determined by enzyme-linked immunosorbent assay. The accumulative data are expressed as mean ± SD from one of two independent experiments. **P<0.01 compared with the vehicle control group. IFN-γ, interferon-γ, IL, interleukin; TNF, tumor necrosis factor.

of CS2164 may be associated with its immunomodulatory activities. Currently, the phase I/II clinical trial of CS2164 in advanced HCC patients (ClinicalTrials.gov ID: NCT03245190) is ongoing. The findings in animal models may provide mechanistic support for this clinical study.

Numerous studies have reported the immunosuppressive role of the VEGF/VEGFR pathway in different immune cells, such as T cells, Tregs, MDSCs, DC, macrophages, etc. [25,26]. For example, VEGF directly suppresses T-cell activation [27] and induces Tregs in patients with cancer through VEGFR2 [28], whereas antiangiogenic antagonists can efficiently reverse these effects [9–12]. Also, VEGF is involved in the accumulation of MDSCs and TAMs in tumor-bearing animals [20,21]. In agreement with these findings, treatment with CS2164 was also found to decrease Tregs, MDSCs, and TAMs in the periphery and tumor microenvironment. Recently, it has been shown that VEGF-C/VEGFR3 signaling promotes tumor lymphangiogenesis and tissue infiltration of naive T cells through the CCL21–CCR7 axis in a melanoma model [24]. This may explain why CS2164 decreased the frequencies of $CD4^+$ and $CD8^+$ T cells in the ascites, but conversely restored those in the periphery. Thus, the immunomodulatory effect of CS2164 is likely through the blockade of the VEGF/VEGFR pathway.

Besides the VEGF/VEGFR pathway, CSF-1/CSF-1R signaling is another nonredundant pathway for the proliferation and infiltration of MDSCs and TAMs [22,23].

Furthermore, inhibition of CSF-1R was found to reduce the recruitment of TAMs and MDSCs and augment the antitumor and antiangiogenic effects of VEGFR2 antibody [29]. Therefore, the decrease in MDSCs and TAMs in the periphery and tumor tissue by CS2164 in this study is possibly because of the combined inhibition of its two major targets: the VEGFR and CSF-1R signaling pathways. In turn, this may further explain the reduction of Tregs in CS2164-treated mice, considering that myeloid cells can modulate the de novo development and induction of Tregs [30]. Although it has been reported in some studies that VEGFR or CSF-1R antagonists could skew the TAM phenotype from immune-inhibitory M2 to immune-stimulatory M1 [31,32], whether CS2164 has this capability is still under further investigation. Nevertheless, the increased proinflammatory cytokine gene expression and protein production by CS2164 reflects the alleviation of immunosuppression in the tumor microenvironment.

With the recent success of immune checkpoint inhibitors, immunotherapy has revolutionized the treatment of cancer. However, 50–80% of patients with tumor for which immune checkpoint inhibitors are indicated do not benefit from these drugs. The intrinsically immunosuppressive tumor microenvironment could probably be one of the major reasons. Our findings provide evidence that CS2164, like other antiangiogenic agents, could not only normalize tumor vasculature but also restore antitumor immunity at least by altering some key components of the tumor microenvironment, which may build up the foundation for combined therapies in future with various immunotherapies, including tumor vaccines, chimeric antigen receptor T cells, and immune checkpoint inhibitors [33].

Acknowledgements

This study was supported by grants from the National Science and Technology Major Projects (2011ZX09102-001-09, 2013ZX09401301, and 2018ZX09301020-003), the Significant Project in Biotech Field from Shenzhen City (GJHS20120820153947138), the Basic Research Projects of Shenzhen Science and Technology Plan (JCYJ20160427185121156), and the Collaborative Innovation Project from Shenzhen Science and Technology Innovation Committee (GJHS20160831155623609).

Conflicts of interest

There are no conflicts of interest.

References

1 Yang JD, Roberts LR. Hepatocellular carcinoma: a global view. *Nat Rev Gastroenterol Hepatol* 2010; **7**:448–458.
2 Hsu CY, Lee YH, Huang YH, Hsia CY, Su CW, Lin HC, *et al.* Ascites in patients with hepatocellular carcinoma: prevalence, associated factors, prognostic impact, and staging strategy. *Hepatol Int* 2013; **7**:188–198.
3 Llovet JM, Ricci S, Mazzaferro V, Hilgard P, Gane E, Blanc JF, *et al.* Sorafenib in advanced hepatocellular carcinoma. *N Engl J Med* 2008; **359**:378–390.
4 Bruix J, Qin S, Merle P, Granito A, Huang YH, Bodoky G, *et al.* Regorafenib for patients with hepatocellular carcinoma who progressed on sorafenib treatment (RESORCE): a randomised, double-blind, placebo-controlled, phase 3 trial. *Lancet* 2017; **389**:56–66.
5 El-Khoueiry AB, Sangro B, Yau T, Crocenzi TS, Kudo M, Hsu C, *et al.* Nivolumab in patients with advanced hepatocellular carcinoma (CheckMate 040): an open-label, non-comparative, phase 1/2 dose escalation and expansion trial. *Lancet* 2017; **389**:2492–2502.
6 Ohm JE, Carbone DP. VEGF as a mediator of tumor-associated immunodeficiency. *Immunol Res* 2001; **23**:263–272.
7 Johnson B, Osada T, Clay T, Lyerly H, Morse M. Physiology and therapeutics of vascular endothelial growth factor in tumor immunosuppression. *Curr Mol Med* 2009; **9**:702–707.
8 Ozao-Choy J, Ma G, Kao J, Wang GX, Meseck M, Sung M, *et al.* The novel role of tyrosine kinase inhibitor in the reversal of immune suppression and modulation of tumor microenvironment for immune-based cancer therapies. *Cancer Res* 2009; **69**:2514–2522.
9 Terme M, Pernot S, Marcheteau E, Sandoval F, Benhamouda N, Colussi O, *et al.* VEGFA–VEGFR pathway blockade inhibits tumor-induced regulatory T-cell proliferation in colorectal cancer. *Cancer Res* 2013; **73**:539–549.
10 Finke JH, Rini B, Ireland J, Rayman P, Richmond A, Golshayan A, *et al.* Sunitinib reverses type-1 immune suppression and decreases T-regulatory cells in renal cell carcinoma patients. *Clin Cancer Res* 2008; **14**:6674–6682.
11 Busse A, Asemissen AM, Nonnenmacher A, Braun F, Ochsenreither S, Stather D, *et al.* Immunomodulatory effects of sorafenib on peripheral immune effector cells in metastatic renal cell carcinoma. *Eur J Cancer* 2011; **47**:690–696.
12 Cabrera R, Ararat M, Xu Y, Brusko T, Wasserfall C, Atkinson MA, *et al.* Immune modulation of effector CD4+ and regulatory T cell function by sorafenib in patients with hepatocellular carcinoma. *Cancer Immunol Immunother* 2013; **62**:737–746.
13 Huang Y, Kim BYS, Chan CK, Hahn SM, Weissman IL, Jiang W. Improving immune-vascular crosstalk for cancer immunotherapy. *Nat Rev Immunol* 2018; **18**:195–203.
14 Zhou Y, Shan S, Li ZB, Xin LJ, Pan DS, Yang QJ, *et al.* CS2164, a novel multi-target inhibitor against tumor angiogenesis, mitosis and chronic inflammation with anti-tumor potency. *Cancer Sci* 2017; **108**:469–477.
15 Wei Q, Zhang D, Yao A, Mai L, Zhang Z, Zhou Q. Design, synthesis, and in vitro and in vivo biological studies of a 3′-deoxythymidine conjugate that potentially kills cancer cells selectively. *PLoS One* 2012; **7**:e52199.
16 Tomayko MM, Reynolds CP. Determination of subcutaneous tumor size in athymic (nude) mice. *Cancer Chemother Pharmacol* 1989; **24**:148–154.
17 Hao C, Shi Y, Yu J, Wei X, Li S, Tong Z. The therapeutic function of the chemokine RANTES on the H22 hepatoma ascites model. *Mol Cell Biochem* 2012; **367**:93–102.
18 Zhang T, Guo W, Yang Y, Liu W, Guo L, Gu Y, *et al.* Loss of SHP-2 activity in CD4+ T cells promotes melanoma progression and metastasis. *Sci Rep* 2013; **3**:2845.
19 Livak KJ, Schmittgen TD. Analysis of relative gene expression data using real-time quantitative PCR and the 2(-Delta Delta C(T)) method. *Methods* 2001; **25**:402–408.
20 Huang Y, Chen X, Dikov MM, Novitskiy SV, Mosse CA, Yang L, *et al.* Distinct roles of VEGFR-1 and VEGFR-2 in the aberrant hematopoiesis associated with elevated levels of VEGF. *Blood* 2007; **110**:624–631.
21 Linde N, Lederle W, Depner S, van Rooijen N, Gutschalk CM, Mueller MM. Vascular endothelial growth factor-induced skin carcinogenesis depends on recruitment and alternative activation of macrophages. *J Pathol* 2012; **227**:17–28.
22 Laoui D, Van Overmeire E, De Baetselier P, Van Ginderachter JA, Raes G. Functional relationship between tumor-associated macrophages and macrophage colony-stimulating factor as contributors to cancer progression. *Front Immunol* 2014; **5**:489.
23 Holmgaard RB, Zamarin D, Lesokhin A, Merghoub T, Wolchok JD. Targeting myeloid-derived suppressor cells with colony stimulating factor-1 receptor blockade can reverse immune resistance to immunotherapy in indoleamine 2,3-dioxygenase-expressing tumors. *EBioMedicine* 2016; **6**:50–58.
24 Fankhauser M, Broggi MAS, Potin L, Bordry N, Jeanbart L, Lund AW, *et al.* Tumor lymphangiogenesis promotes T cell infiltration and potentiates immunotherapy in melanoma. *Sci Transl Med* 2017; **9**:eaal4712.
25 Li YL, Zhao H, Ren XB. Relationship of VEGF/VEGFR with immune and cancer cells: staggering or forward?. *Cancer Biol Med* 2016; **13**:206–214.
26 Yang J, Yan J, Liu B. Targeting VEGF/VEGFR to modulate antitumor immunity. *Front Immunol* 2018; **9**:978.
27 Gavalas NG, Tsiatas M, Tsitsilonis O, Politi E, Ioannou K, Ziogas AC, *et al.* VEGF directly suppresses activation of T cells from ascites secondary

to ovarian cancer via VEGF receptor type 2. *Br J Cancer* 2012; **107**:1869–1875.
28 Wada J, Suzuki H, Fuchino R, Yamasaki A, Nagai S, Yanai K, *et al.* The contribution of vascular endothelial growth factor to the induction of regulatory T-cells in malignant effusions. *Anticancer Res* 2009; **29**:881–888.
29 Priceman SJ, Sung JL, Shaposhnik Z, Burton JB, Torres-Collado AX, Moughon DL, *et al.* Targeting distinct tumor-infiltrating myeloid cells by inhibiting CSF-1 receptor: combating tumor evasion of antiangiogenic therapy. *Blood* 2010; **115**:1461–1471.
30 Gabrilovich DI, Ostrand-Rosenberg S, Bronte V. Coordinated regulation of myeloid cells by tumours. *Nat Rev Immunol* 2012; **12**:253–268.
31 Huang Y, Yuan J, Righi E, Kamoun WS, Ancukiewicz M, Nezivar J, *et al.* Vascular normalizing doses of antiangiogenic treatment reprogram the immunosuppressive tumor microenvironment and enhance immunotherapy. *Proc Natl Acad Sci USA* 2012; **109**:17561–17566.
32 Pyonteck SM, Akkari L, Schuhmacher AJ, Bowman RL, Sevenich L, Quail DF, *et al.* CSF-1R inhibition alters macrophage polarization and blocks glioma progression. *Nat Med* 2013; **19**:1264–1272.
33 Fukumura D, Kloepper J, Amoozgar Z, Duda DG, Jain RK. Enhancing cancer immunotherapy using antiangiogenics: opportunities and challenges. *Nat Rev Clin Oncol* 2018; **15**:325–340.